Surgical Triplet Recognition via Diffusion Model

Daochang Liu[1], Axel Hu[1], Mubarak Shah[2], Chang Xu[1]

[1] School of Computer Science, Faculty of Engineering, The University of Sydney
[2] Center for Research in Computer Vision, University of Central Florida
{daochang.liu, xintao.hu, c.xu}@sydney.edu.au
shah@crcv.ucf.edu

Abstract. Surgical triplet recognition is an essential building block to enable next-generation context-aware operating rooms. The goal is to identify the combinations of instruments, verbs, and targets presented in surgical video frames. In this paper, we propose *DiffTriplet*, a new generative framework for surgical triplet recognition employing the diffusion model, which predicts surgical triplets via iterative denoising. To handle the challenge of triplet association, two unique designs are proposed in our diffusion framework, i.e., association learning and association guidance. During training, we optimize the model in the joint space of triplets and individual components to capture the dependencies among them. At inference, we integrate association constraints into each update of the iterative denoising process, which refines the triplet prediction using the information of individual components. Experiments on the CholecT45 and CholecT50 datasets show the superiority of the proposed method in achieving a new state-of-the-art performance for surgical triplet recognition. Our codes will be released.

Keywords: Surgical action triplet · Surgical workflow · Diffusion model.

1 Introduction

Surgical workflow analysis is a pivotal topic in surgical data science [11], which facilitates intraoperative decision making and postoperative skill assessment [10]. The concept of surgical action triplet [13] has emerged as an intriguing representation that provides fine-grained information about procedural activities and interactions within the surgical scene. The goal is to identify triplets of <*instrument*, *verb*, *target*> by analyzing surgical videos captured by minimally invasive devices. This task has been studied either as a recognition problem where each video frame is classified into categories of triplets [12], or as a detection task which additionally pinpoints the spatial location of the triplets [16,20]. This paper focuses on the recognition of surgical action triplets.

Previous works on surgical triplet recognition have explored various models spanning from convolutional neural networks [13,3,17], recurrent neural networks [8], graph neural networks [1,23,21], to transformers [15,25]. Rendezvous [15,19] is a milestone work that employs an instrument-centric attention mechanism, while Xi *et al.* [24] take a verb-centric approach using verb prompts with vision-language models. Researchers have also investigated on reducing the learning complexity of surgical triplets using progressive task disentanglement [2] or knowledge distillation techniques [5,25]. Unlike these previous works, this paper proposes a fundamentally new framework, *DiffTriplet*,

which tackles surgical triplet recognition in a generative learning way using the diffusion model. The core idea is to learn to denoise noisy triplets in training and iteratively predict triplets by denoising from pure noise at inference.

Our diffusion-based framework is uniquely designed to address one of the key challenges regarding surgical triplets, i.e., the association of triplet components. A surgical triplet comprises an instrument, a verb, and a target, where the association among them is an intrinsic property. On one hand, the three individual components are interdependent, which means that the occurrence of one component may rely on other components. For example, the action verb *<retract>* is more likely to be operated using the instrument *<grasper>*, and the usual targets for this pair are *<gallbladder>* and *<liver>* if the specialty is cholecystectomy. On the other hand, the triplet shows strong prior dependency on the individual components since the triplet classes, e.g. *<grasper, retract, liver>*, are composited from the individual ones by definition. The search space of the triplet will be greatly narrowed down if one of the individual components can be determined. For instance, if the instrument is *<grasper>*, the possible triplets will be only those related to this instrument. Therefore, how to correctly build the association is essential for surgical triplet recognition. To handle the challenge mentioned above, we propose two novel designs in our diffusion framework, which are *association learning in training* and *association guidance at inference*. During the training process, our model learns to denoise in the joint space of triplets, instruments, verbs, and targets, so that the dependency relationships among triplets and individual components can be naturally captured by the generative learning capability of the diffusion model. During the inference process, we propose an association guidance method to enforce the consistency between the predicted triplets and the predicted individual components, by incorporating the dependency constraints into the inference process of the diffusion model. These two designs help our diffusion model better exploit the triplet association during both training and inference.

To validate our proposed method, we conduct comprehensive experiments on the CholecT45 [12] and CholecT50 [15] datasets, where we achieve the state-of-the-art performance under the official cross-validation setting with 40.2% average precision on CholecT45 and 40.3% on CholecT50. Experiments also show that the proposed association learning and association guidance bring evident improvements. In summary, our contributions are three-fold:

1) We propose a new generative framework for surgical triplet recognition which is the first diffusion model for surgical video understanding to our knowledge.

2) We propose the joint space learning and the association guidance to explicitly enhance the correct triplet associations during both training and inference.

3) We conduct extensive experiments to demonstrate our state-of-the-art performance.

2   Method

The task of surgical triplet recognition is to take a surgical video as input and output the triplets in each frame. A triplet is a combination of instrument, verb, and target. There can be a single triplet, multiple triplets, or no triplet in each frame. In the following, we begin with the background knowledge of diffusion models and a basic diffusion

framework for triplet recognition. We then introduce the designs of joint space learning and association guidance to handle the challenge of triplet association.
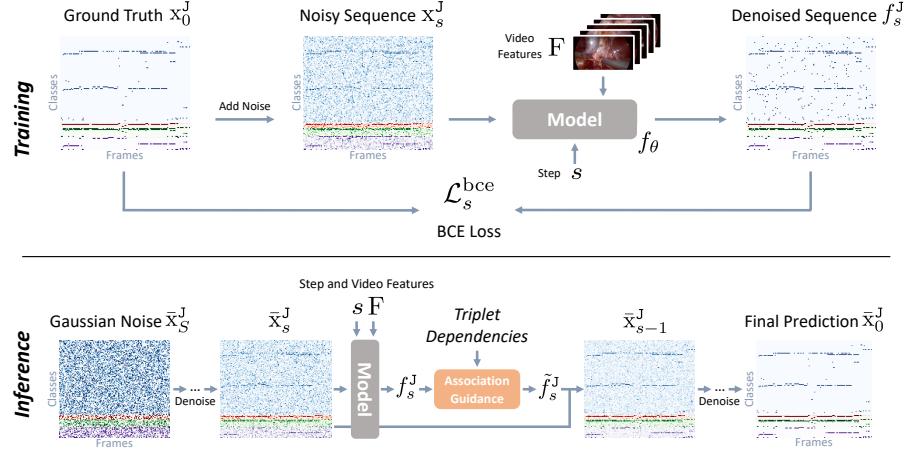

Fig. 1. Illustration of our *DiffTriplet* framework. During training, the model is trained to denoise noisy sequences in the joint space of triplets and individual components. During inference, the model iteratively generates the prediction by gradually reducing the noise starting from a pure noise sequence. In the joint space matrices $x^J, \bar{x}^J$, the blue rows are triplets $x^{IVT}, \bar{x}^{IVT}$, red rows are instruments $x^I, \bar{x}^I$, green rows are verbs $x^V, \bar{x}^V$, and purple rows are targets $x^T, \bar{x}^T$. Darker colors means higher probabilities. For the model f_θ, a causal temporal model is used.

2.1 Preliminaries

Diffusion models [4,6,22,18] have witnessed remarkable success as a new type of generative model, which have also shown potential for video analysis [9] in computer vision. The diffusion model consists of two complementary processes, namely the forward process and the reverse process, to simulate the true distribution $q(x_0)$ with a model distribution $p_\theta(x_0)$. Specifically, the forward process gradually adds noise into the clean data $x_0 \sim q(x_0)$ and produces a series of noisy data $x_1, x_2, ..., x_S$, where S is the total steps of the process. The reverse process generates new data starting from a pure Gaussian noise $\bar{x}_S$ and iteratively denoising the data along steps from $\bar{x}_{S-1}, \bar{x}_{S-2}, ...$ to $\bar{x}_0 \sim p_\theta(x_0)$ at the end.

2.2 Diffusion Triplet Recognition

Our diffusion framework for triplet recognition conducts generative learning on triplet sequences. Given a surgical video with L frames, we denote the ground-truth triplets as a binary sequence $x_0^{IVT} \in \{0, 1\}^{L \times C_{IVT}}$, where C_{IVT} is the number of triplet classes.

Training. During training, the forward process gradually corrupts the ground-truth triplet sequence x_0^{IVT} to $x_1^{\text{IVT}}, x_2^{\text{IVT}}, ..., x_S^{\text{IVT}}$ with varying noise levels. Formally, at step s, the noisy triplet sequence $x_s^{\text{IVT}} \in [0,1]^{L \times C_{\text{IVT}}}$ is obtained in a closed form,

$$x_s^{\text{IVT}} = \sqrt{\alpha_s} x_0^{\text{IVT}} + \epsilon \sqrt{1 - \alpha_s}, \tag{1}$$

where ϵ is a random Gaussian noise and α_s is the schedule parameter defining the noise levels [22]. The resultant sequence is clipped within the range $[0,1]$. We use a step-dependent neural network $f_\theta(x_s^{\text{IVT}}, s, \text{F})$ to model the data distribution of triplet sequences by restoring the clean triplet sequence x_0^{IVT} from the noisy version x_s^{IVT}. The inputs of the network include the noisy sequence x_s^{IVT}, the embedding of step s, and pre-extracted video features $\text{F} \in \mathbb{R}^{L \times D}$ with L frames and D dimensions. Using video features as conditional inputs for our diffusion model is crucial to build the mapping between surgical video and triplets in this video. The network f_θ is then trained with a binary cross entropy (BCE) loss between the network output and the clean triplet sequence x_0^{IVT}. In each training iteration, the step $s \in \{1, 2, ..., S\}$ is selected randomly. Note that we follow the convention of triplet recognition and use a *causal* model for f_θ where the prediction of each frame can only utilize the information not after this frame.

Inference. Once the network f_θ is optimized, the reverse process starts from pure Gaussian noise $\bar{x}_S^{\text{IVT}}$ and iteratively reduces the noise through steps $\bar{x}_{S-1}^{\text{IVT}}, \bar{x}_{S-2}^{\text{IVT}}, ...$ to obtain the final prediction $\bar{x}_0^{\text{IVT}}$ at the last step. We use the bar notation $\bar{\cdot}$ to differentiate the variables during inference from those in training. At each inference step, the iteration adopts the update rule of the reverse sampling of diffusion models [22],

$$\begin{aligned} \bar{x}_{s-1}^{\text{IVT}} = & \sqrt{\alpha_{s-1}} f_\theta(\bar{x}_s^{\text{IVT}}, s, \text{F}) + \\ & \sqrt{1 - \alpha_{s-1} - \sigma_s^2} \frac{\bar{x}_s^{\text{IVT}} - \sqrt{\alpha_s} f_\theta(\bar{x}_s^{\text{IVT}}, s, \text{F})}{\sqrt{1 - \alpha_s}} + \sigma_s \epsilon, \end{aligned} \tag{2}$$

where ϵ is a random Gaussian noise, σ_s is a variance schedule depending on the schedule parameter α_s. The output $\bar{x}_0^{\text{IVT}}$ in the last step is used as the final prediction since it is guaranteed to be close to the true triplets x_0^{IVT} according to diffusion model theories [6].

2.3 Association Learning in Joint Space

To better establish the association of triplet components, we first enhance the association learning by transforming our diffusion model from learning solely in the triplet space x_0^{IVT} to learning in a joint space x_0^{J} of both triplets and individual components. Our framework is illustrated in Fig. 1.

Joint space construction. Recall that we conduct the forward and reverse processes on the triplet sequence x_0^{IVT} in Sec 2.2, and now we re-formulate the processes on a sequence $x_0^{\text{J}} \in \{0,1\}^{L \times C_{\text{J}}}$ in the joint space. Specifically, the joint space $x_0^{\text{J}} := x_0^{\text{IVT}} \oplus x_0^{\text{I}} \oplus x_0^{\text{V}} \oplus x_0^{\text{T}}$ is constructed by combining the triplets with the corresponding instruments, verbs, and targets. Let $x_0^{\text{I}} \in \{0,1\}^{L \times C_{\text{I}}}$, $x_0^{\text{V}} \in \{0,1\}^{L \times C_{\text{V}}}$, $x_0^{\text{T}} \in \{0,1\}^{L \times C_{\text{T}}}$ represent the binary ground-truth sequences for the instruments, verbs, and targets respectively, where $C_{\text{I}}, C_{\text{V}}, C_{\text{T}}$ are the numbers of classes. We choose $\oplus$ as a concatenation operation in our current implementation and thus the dimension of the joint space C_{J} adheres to $C_{\text{J}} = C_{\text{IVT}} + C_{\text{I}} + C_{\text{V}} + C_{\text{T}}$.

Joint space learning. In the joint space, we reformulate the forward process in Eq. 1 to the following one to obtain the noisy sequence $x_s^J \in [0,1]^{L \times C_J}$ at step s,

$$x_s^J = \sqrt{\alpha_s} x_0^J + \epsilon \sqrt{1 - \alpha_s}. \tag{3}$$

We then replace the input of the network from the sequence in the triplet space x_s^{IVT} with the one in the joint space x_s^J. The network output $f_\theta(x_s^J, s, F)$ is denoted as $f_s^J \in [0,1]^{L \times C_J}$ for brevity. We train the network to denoise the noisy sequence by minimizing a BCE loss between the output f_s^J and the ground-truth in the joint space x_0^J,

$$\mathcal{L}_s^{bce} = -\frac{1}{LC_J} \sum_{i=1}^{L} \sum_{c=1}^{C_J} x_{0|i,c}^J \log f_{s|i,c}^J + (1 - x_{0|i,c}^J)\log(1 - f_{s|i,c}^J), \tag{4}$$

where $x_{0|i,c}^J$ and $f_{s|i,c}^J$ are the ground truth and prediction elements for frame i and class c respectively. The reverse process for inference in Eq. 2 is updated correspondingly,

$$\begin{aligned} \bar{x}_{s-1}^J = &\sqrt{\alpha_{s-1}} f_\theta(\bar{x}_s^J, s, F) + \\ &\sqrt{1 - \alpha_{s-1} - \sigma_s^2} \frac{\bar{x}_s^J - \sqrt{\alpha_s} f_\theta(\bar{x}_s^J, s, F)}{\sqrt{1 - \alpha_s}} + \sigma_s \epsilon. \end{aligned} \tag{5}$$

Such generative modeling using the diffusion model in the joint space naturally encourages the model to capture the dependencies among the triplets and the individual components during training. Moreover, it also enables the injection of explicit triplet dependencies in the inference process with an association guidance we will introduce in the following section.

2.4 Association Guidance at Inference

Our second design to enhance the correct triplet association is a guidance method improving the inference process. This is based on a key observation prevalent in existing triplet recognition models, where the models tend to have better recognition performance for individual components than the compositional triplet, potentially due to the higher dimensionality of triplet. This phenomenon also exists in our diffusion model. Therefore, we propose to utilize the individual component predictions to guide the triplet prediction and rectify errors by enforcing triplet association constraints.

To this end, we first represent the constraints with three dependency matrices $M_I \in \{0,1\}^{C_I \times C_{IVT}}$, $M_V \in \{0,1\}^{C_V \times C_{IVT}}$, $M_T \in \{0,1\}^{C_T \times C_{IVT}}$ capturing the relations between triplets and instruments, verbs, targets respectively[3]. The matrices register the possibility of triplets when each component occurs. For example, M_I represents the possible triplets when each class of instrument appears. These matrices can be obtained from the label mapping that defines the triplet classes or summarized from the statistics of the training dataset. To inject the constraints, in each inference step, we decompose the model output in the joint space f_s^J back into individual spaces $f_s^{IVT}, f_s^I, f_s^V, f_s^T$,

$$f_s^J \Rightarrow f_s^{IVT} \in [0,1]^{L \times C_{IVT}}, f_s^I \in [0,1]^{L \times C_I}, f_s^V \in [0,1]^{L \times C_V}, f_s^T \in [0,1]^{L \times C_T}, \tag{6}$$

---

[3] Please refer to the supplementary material for visualized matrices.

where the decomposition a reversed operation of the previous concatenation. Using the individual outputs, a guidance term $g_s \in [0,1]^{L \times C_{\text{IVT}}}$ for the triplet prediction is computed incorporating the dependency between the triplet and the components,

$$g_s = (f_s^{\text{I}} \otimes M_{\text{I}}) \odot (f_s^{\text{V}} \otimes M_{\text{V}}) \odot (f_s^{\text{T}} \otimes M_{\text{T}}), \tag{7}$$

where $\otimes$ is matrix multiplication and $\odot$ is element-wise product. Intuitively, the guidance term in Eq. 7 represents the possible triplets inferred from the predicted individual components, aggregated over instrument, verbs, and targets. Then we compute a linear combination of the original triplet prediction f_s^{IVT} and the prediction combining the guidance term to steer the inference process with the triplet dependencies injected,

$$\tilde{f}_s^{\text{IVT}} := (1 - \omega) f_s^{\text{IVT}} + \omega g_s \odot f_s^{\text{IVT}}, \tag{8}$$

where ω is a hyper-parameter controlling the guidance scale. The updated triplet prediction $\tilde{f}_s^{\text{IVT}}$ alleviates the errors in f_s^{IVT} by employing the individual components that are usually better recognized. The joint space is then re-composed using the updated triplet prediction, namely, $\tilde{f}_s^{\text{J}} := \tilde{f}_s^{\text{IVT}} \oplus f_s^{\text{I}} \oplus f_s^{\text{V}} \oplus f_s^{\text{T}}$. The overall inference process is kept similar to Eq. 5 but only replacing f_s^{J} with the updated $\tilde{f}_s^{\text{J}}$. Our association guidance improves the inference process through the triplet association constraints.

3   Experiments

Datasets. We conduct experiments on the benchmarks for surgical triplet recognition, i.e., CholecT50 [15] and CholecT45 [12] datasets. The CholecT50 dataset consists of 50 videos of cholecystectomy surgeries captured by laparoscopic cameras, and the CholecT45 dataset is a subset with 45 videos. The data has been used in the MICCAI EndoVis CholecTriplet challenges [12,16]. Both datasets provide annotations for 100 classes of surgical triplets ($C_{\text{IVT}} = 100$), 6 classes of instruments ($C_{\text{I}} = 6$), 10 classes of verbs ($C_{\text{V}} = 10$), and 15 classes of targets ($C_{\text{T}} = 15$). The videos are down-sampled to 1 fps and have 2000 frames per video on average.

Setup. Various experimental settings with different data splits have been employed in previous works [14], making it challenging to compare across methods. Therefore, we base our experiments on a consistent setup, using the five-fold **cross-validation setting recommended for research use** in the future, as described by the dataset owner in [14]. We also use the official data splits [14]. To evaluate recognition performance, the recommended Average Precision metrics [14] are computed for the triplet (AP_{IVT}), three individual components (AP_{I}, AP_{V}, AP_{T}), and the two instrument-related pairs (AP_{IV}, AP_{IT}). We use the official `ivtmetrics` library [14] to compute the metrics.

Implementation Details. The triplet sequences are normalized to $[-1, 1]$ when adding and removing noise. Our model f_θ uses the architecture of the encoder in ASFormer [26], which incorporates both temporal convolutions and attentions to enable temporal reasoning across frames. We modify the model to be *causal* to follow previous conventions regarding the causality constraint [12] that restricts the model from utilizing future frames. This is achieved by changing the temporal convolutions to causal convolutions [7] and limiting the attention within the receptive fields of the causal convolutions.

Table 1. Comparison to the state-of-the-art. We follow the official recommended cross-validation. †: Results reported in original papers use the Rendezvous setting [15] instead of cross-validation. ‡: Results reported in original papers use the Challenge setting [14] instead of cross-validation. §: Extra textual information and language models are used. ∗: Results obtained using public codes. Gray: Results should be compared with caution due to different settings. Empty cells mean results are not reported in original papers. F_{RDV}: Rendezvous features. F_{SDSwin}: SDSwin features.

Method	AP_I	AP_V	AP_T	AP_{IV}	AP_{IT}	AP_{IVT}
CholecT45						
Tripnet [13,1]	89.9±1.0	59.9±0.9	37.4±1.5	31.8±4.1	27.1±2.8	24.4±4.7
Attention Triplet [15,1]	89.1±2.1	61.2±0.6	40.3±1.2	33.0±2.9	29.4±1.2	27.2±2.7
Rendezvous [15,1]	89.3±2.1	62.0±1.3	40.0±1.4	34.0±3.3	30.8±2.1	29.4±2.8
ConceptNet-ViT [1]	88.3±1.4	65.1±3.9	43.8±3.1	33.7±3.2	33.4±3.2	30.6±1.9
RiT [19]	88.6±2.6	64.0±2.5	43.4±1.4	38.3±3.5	36.9±1.0	29.7±2.6
TDN [2]	91.2±1.9	65.3±2.8	43.7±1.6	-	-	33.8±2.5
MT4MTL-KD (No Ensemble) [5]	93.1±2.1	**71.8**±3.4	48.8±3.8	44.9±2.4	43.1±2.0	37.1±0.5
SDSwin (No Ensemble) [25]	-	-	-	-	-	36.1± -
Ours (F_{RDV})	91.8±1.8	66.3±1.4	45.5±1.9	42.7±4.6	42.2±1.9	35.0±3.2
Ours (F_{SDSwin})	**95.1**±1.6	71.1±1.3	**51.7**±3.3	**46.2**±3.9	**47.4**±2.4	**40.2**±1.9
CholecT50						
Rendezvous [15,14]	89.4±2.0	60.4±2.8	40.3±2.2	34.5±2.8	31.8±1.0	29.4±2.5
†, § Forest GCN [23]	93.1± -	60.1± -	40.2± -	36.2± -	37.5± -	36.7± -
†, § Chain-of-Look [24]	94.1± -	62.5± -	41.9± -	41.7± -	39.5± -	38.2± -
‡ MoCoV2 [17]	-	-	-	-	-	35.7± -
‡ MT-FiST [8]	82.1± -	51.5± -	45.5± -	37.1± -	43.1± -	35.8± -
‡ MT4MTL-KD (No Ensemble) [5]	86.8± -	57.5± -	46.3± -	39.5± -	41.3± -	37.2± -
‡ SDSwin (No Ensemble) [25]	-	-	-	-	-	37.3± -
∗ SDSwin (No Ensemble) [25]	-	-	-	-	-	36.2±1.9
Ours (F_{RDV})	92.6±1.7	66.2±2.1	45.0±2.1	42.5±4.3	42.4±1.3	35.1±2.7
Ours (F_{SDSwin})	**95.3**±1.4	**70.9**±0.8	**53.1**±2.6	**46.4**±4.1	**48.2**±1.8	**40.3**±2.5

The model is of 2 layers with 256 feature maps. We set the total number of diffusion step $S = 1000$ and use the DDIM sampling rule [22] with 8 steps at inference. The model is trained using the Adam optimizer with a learning rate of 5e-5, a weight decay of 1e-5, a batch size of 1, and 500 epochs. We set the guidance scale $\omega = 1.0$ in our experiments. The choice of the video features F is flexible. In practice, given the code availability, we extract video features F from intermediate layer of pre-trained Rendezvous (RDV) models [15] ($D = 2500$) or pre-trained non-ensemble models of self-distilled-swin (SDSwin) [25] ($D = 1024$). The dependency matrices are obtained from the label mapping coming along with the dataset [15]. Our code is implemented using PyTorch. The models are trained within one hour using a single NVIDIA V100 GPU. Our full codes and pre-trained models will be released.

3.1 Results

Comparison to the State-of-the-Art. Table 1 presents a comparison between our results and previous results reported in the literature on the two datasets. For previous

Table 2. Ablation studies on CholecT50 cross-validation using F_{RDV}. We also provide a comparison between the performance of the (online) causal model and an (offline) acausal model.

Method	AP_I	AP_V	AP_T	AP_{IV}	AP_{IT}	AP_{IVT}
a. Impact of Joint Space Learning						
Rendezvous Baseline [15,14]	89.4±2.0	60.4±2.8	40.3±2.2	34.5±2.8	31.8±1.0	29.4±2.5
Ours (w/o Joint Space)	-	-	-	40.3±4.8	39.9±1.6	32.6±2.2
Ours (with Joint Space)	92.6±1.7	66.2±2.1	45.0±2.1	42.5±4.3	42.4±1.3	35.1±2.7
b. Different Combinations of I, V, T for the Joint Space						
Ours (IVT)	-	-	-	40.3±4.8	39.9±1.6	32.6±2.2
Ours (IVT + I)	92.5±1.6	-	-	41.7±4.5	40.2±1.3	33.0±2.2
Ours (IVT + V)	-	65.7±2.6	-	40.5±5.0	40.5±1.8	32.9±2.5
Ours (IVT + T)	-	-	44.1±2.2	40.6±4.7	39.5±1.6	32.3±2.0
Ours (IVT + IV)	-	-	-	41.0±4.4	40.2±1.6	32.9±2.3
Ours (IVT + IT)	-	-	-	41.0±5.1	40.4±1.5	32.8±2.3
Ours (IVT + I + V + T)	92.6±1.7	66.2±2.1	45.0±2.1	42.5±4.3	42.4±1.3	35.1±2.7
c. Impact of Association Guidance						
Ours (Scale $\omega = 0.00$)	92.6±1.7	66.2±2.1	45.0±2.1	41.2±4.3	40.9±1.4	33.3±2.2
Ours (Scale $\omega = 0.50$)	92.6±1.7	66.2±2.1	45.0±2.1	41.7±4.5	41.4±1.4	33.9±2.3
Ours (Scale $\omega = 1.00$)	92.6±1.7	66.2±2.1	45.0±2.1	42.5±4.3	42.4±1.3	35.1±2.7
d. Causal Model and Acausal Model						
Ours (Causal)	92.6±1.7	66.2±2.1	45.0±2.1	42.5±4.3	42.4±1.3	35.1±2.7
Ours (Acausal)	94.0±1.1	68.2±2.2	46.3±3.0	44.9±4.8	44.7±2.1	37.2±3.7

methods using ensemble models [25,5], we present the results of their non-ensemble models to facilitate direct comparison. It can be seen that our proposed method evidently improves the state-of-the-art performance (40.2 vs. 37.1 AP_{IVT} on CholecT45), validating the efficacy of our diffusion-based framework for triplet recognition. In Table 1, we also include results previously reported under the Rendezvous setting [15] and the Challenge setting [14], not officially recommended for research [14], for readers' reference but with caution. Our method only has a slight computational overhead, with an inference speed of 16.9 fps, compared to 19.1 fps for Rendezvous [15], both measured on the same device with a NVIDIA T4 GPU.

Ablation Studies. We present ablation studies in Table 2 to validate each design.

Joint space learning. Firstly, the importance of the proposed joint space learning is investigated in Table 2a. Compared to the baseline, our diffusion model achieves notable gain (32.6 vs. 29.4 AP_{IVT}), which is further improved by learning in the joint space (35.1 vs. 32.6 AP_{IVT}). We further provide the results using different combinations regarding the joint space in Table 2b. Other combinations (IVT + I/V/T/IV/IT) are not as good as our proposed space (IVT + I + V + T), due to the partial association.

Association Guidance. Secondly, we provides the results with difference scales of the association guidance in Table 2c, where $\omega = 1.00$ means full guidance and $\omega = 0.00$ means no guidance. The guidance effectively strengthens the triplet association and obtains better performance (35.1 vs. 33.3 AP_{IVT}). Metrics for individual components are the same across scales since they are not affected by the guidance.

Causal vs. Acausal. Thirdly, in Table 2d, we additionally explore how the model performs when the causality constraint is removed. We compare the results of the causal model and an acausal model that employing the normal version of convolutions and attentions. It is encouraging that the performance is further improved when the acausal model is used (37.2 vs. 35.1 AP_{IVT}), showing the potential of our method not only for online analysis but also more accurate offline analysis for surgical videos.

Inference Steps. In Table 3, we present the results using different numbers of inference steps. This experiment shows that the result is stable across different inference steps. The computational cost increases linearly with the number of inference steps. Therefore, we use 8 steps to achieve a balance between accuracy and speed.

Table 3. Results using different inference steps on CholecT50 cross-validation with F_{RDV}.

Steps	AP_I	AP_V	AP_T	AP_{IV}	AP_{IT}	AP_{IVT}
Steps = 1	91.9±1.7	65.4±2.3	44.6±2.2	41.9±4.4	41.5±1.7	34.3±3.0
Steps = 2	92.5±1.7	65.9±2.3	44.9±2.2	42.4±4.4	42.3±1.4	35.0±2.9
Steps = 4	92.6±1.7	66.1±2.1	45.1±2.1	42.6±4.3	42.4±1.4	35.1±2.7
Steps = 8	92.6±1.7	66.2±2.1	45.0±2.1	42.5±4.3	42.4±1.3	35.1±2.7
Steps = 16	92.6±1.7	66.1±2.1	45.0±2.1	42.5±4.3	42.4±1.3	35.0±2.7

4   Conclusion

This paper proposes a generative framework for surgical triplet recognition using a diffusion model with the joint space learning and the association guidance. Future works can explore more forms of the triplet dependencies, such as the soft dependencies summarized from training statistics, and the inter-component dependencies to refine the predictions of the individual components. It is also promising to design an association guidance with a progressive hierarchy from components to pairs and finally to triplets.

References

1. Ban, Y., Eckhoff, J.A., Ward, T.M., Hashimoto, D.A., Meireles, O.R., Rus, D., Rosman, G.: Concept graph neural networks for surgical video understanding. IEEE Transactions on Medical Imaging (2023)
2. Chen, Y., He, S., Jin, Y., Qin, J.: Surgical activity triplet recognition via triplet disentanglement. In: International Conference on Medical Image Computing and Computer-Assisted Intervention (MICCAI). pp. 451–461. Springer (2023)

3. Cheng, Y., Liu, L., Wang, S., Jin, Y., Schönlieb, C.B., Aviles-Rivero, A.I.: Why deep surgical models fail?: Revisiting surgical action triplet recognition through the lens of robustness. In: International Workshop on Trustworthy Machine Learning for Healthcare. pp. 177–189. Springer (2023)
4. Dhariwal, P., Nichol, A.: Diffusion models beat GANs on image synthesis. The Conference on Neural Information Processing Systems (NeurIPS) (2021)
5. Gui, S., Wang, Z., Chen, J., Zhou, X., Zhang, C., Cao, Y.: MT4MTL-KD: A multi-teacher knowledge distillation framework for triplet recognition. IEEE Transactions on Medical Imaging (2023)
6. Ho, J., Jain, A., Abbeel, P.: Denoising diffusion probabilistic models. The Conference on Neural Information Processing Systems (NeurIPS) (2020)
7. Lea, C., Flynn, M.D., Vidal, R., Reiter, A., Hager, G.D.: Temporal convolutional networks for action segmentation and detection. In: Proceedings of the IEEE/CVF Conference on Computer Vision and Pattern Recognition (CVPR). pp. 156–165 (2017)
8. Li, Y., Xia, T., Luo, H., He, B., Jia, F.: MT-FiST: A multi-task fine-grained spatial-temporal framework for surgical action triplet recognition. IEEE Journal of Biomedical and Health Informatics (2023)
9. Liu, D., Li, Q., Dinh, A.D., Jiang, T., Shah, M., Xu, C.: Diffusion action segmentation. In: Proceedings of the IEEE/CVF International Conference on Computer Vision (ICCV). pp. 10139–10149 (2023)
10. Liu, D., Li, Q., Jiang, T., Wang, Y., Miao, R., Shan, F., Li, Z.: Towards unified surgical skill assessment. In: Proceedings of the IEEE/CVF Conference on Computer Vision and Pattern Recognition (CVPR). pp. 9522–9531 (2021)
11. Maier-Hein, L., Eisenmann, M., Sarikaya, D., März, K., Collins, T., Malpani, A., Fallert, J., Feussner, H., Giannarou, S., Mascagni, P., et al.: Surgical data science–from concepts toward clinical translation. Medical Image Analysis **76**, 102306 (2022)
12. Nwoye, C.I., Alapatt, D., Yu, T., Vardazaryan, A., Xia, F., Zhao, Z., Xia, T., Jia, F., Yang, Y., Wang, H., et al.: CholecTriplet2021: A benchmark challenge for surgical action triplet recognition. Medical Image Analysis **86**, 102803 (2023)
13. Nwoye, C.I., Gonzalez, C., Yu, T., Mascagni, P., Mutter, D., Marescaux, J., Padoy, N.: Recognition of instrument-tissue interactions in endoscopic videos via action triplets. In: International Conference on Medical Image Computing and Computer-Assisted Intervention (MICCAI). pp. 364–374. Springer (2020)
14. Nwoye, C.I., Padoy, N.: Data splits and metrics for benchmarking methods on surgical action triplet datasets. arXiv preprint arXiv:2204.05235 (2022)
15. Nwoye, C.I., Yu, T., Gonzalez, C., Seeliger, B., Mascagni, P., Mutter, D., Marescaux, J., Padoy, N.: Rendezvous: Attention mechanisms for the recognition of surgical action triplets in endoscopic videos. Medical Image Analysis **78**, 102433 (2022)
16. Nwoye, C.I., Yu, T., Sharma, S., Murali, A., Alapatt, D., Vardazaryan, A., Yuan, K., Hajek, J., Reiter, W., Yamlahi, A., et al.: CholecTriplet2022: Show me a tool and tell me the triplet–an endoscopic vision challenge for surgical action triplet detection. arXiv preprint arXiv:2302.06294 (2023)
17. Ramesh, S., Srivastav, V., Alapatt, D., Yu, T., Murali, A., Sestini, L., Nwoye, C.I., Hamoud, I., Sharma, S., Fleurentin, A., et al.: Dissecting self-supervised learning methods for surgical computer vision. Medical Image Analysis **88**, 102844 (2023)
18. Rombach, R., Blattmann, A., Lorenz, D., Esser, P., Ommer, B.: High-resolution image synthesis with latent diffusion models. In: Proceedings of the IEEE/CVF Conference on Computer Vision and Pattern Recognition (CVPR) (2022)
19. Sharma, S., Nwoye, C.I., Mutter, D., Padoy, N.: Rendezvous in time: an attention-based temporal fusion approach for surgical triplet recognition. International Journal of Computer Assisted Radiology and Surgery (2023)

20. Sharma, S., Nwoye, C.I., Mutter, D., Padoy, N.: Surgical action triplet detection by mixed supervised learning of instrument-tissue interactions. In: International Conference on Medical Image Computing and Computer-Assisted Intervention (MICCAI). pp. 505–514. Springer (2023)
21. Sista, R., Sathish, R., Agrawal, R., De, U., Chakrabarti, P., Sheet, D.: I'm GROOT: a multi head multi graph network recognizing surgical action triplets. In: Proceedings of the Thirteenth Indian Conference on Computer Vision, Graphics and Image Processing (2022)
22. Song, J., Meng, C., Ermon, S.: Denoising diffusion implicit models. The International Conference on Learning Representations (ICLR) (2021)
23. Xi, N., Meng, J., Yuan, J.: Forest graph convolutional network for surgical action triplet recognition in endoscopic videos. IEEE Transactions on Circuits and Systems for Video Technology **32**(12), 8550–8561 (2022)
24. Xi, N., Meng, J., Yuan, J.: Chain-of-Look prompting for verb-centric surgical triplet recognition in endoscopic videos. In: Proceedings of the 31st ACM International Conference on Multimedia. pp. 5007–5016 (2023)
25. Yamlahi, A., Tran, T.N., Godau, P., Schellenberg, M., Michael, D., Smidt, F.H., Nölke, J.H., Adler, T.J., Tizabi, M.D., Nwoye, C.I., et al.: Self-distillation for surgical action recognition. In: International Conference on Medical Image Computing and Computer-Assisted Intervention (MICCAI). pp. 637–646. Springer (2023)
26. Yi, F., Wen, H., Jiang, T.: ASFormer: Transformer for action segmentation. In: The British Machine Vision Conference (BMVC) (2021)
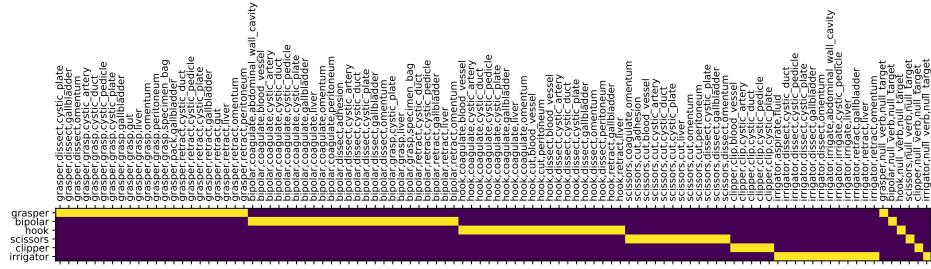
5   Supplementary Material

Fig. 2. Visualization of the dependency matrix $M_{\mathrm{I}} \in \{0, 1\}^{C_{\mathrm{I}} \times C_{\mathrm{IVT}}}$. Yellow cells (value=1) are the possible associations between the triplet and the instrument. Blue cells (value=0) are the impossible associations between the triplet and the instrument.
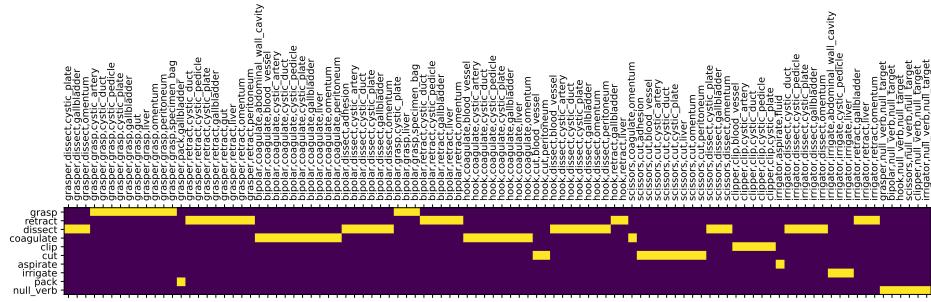

Fig. 3. Visualization of the dependency matrix $M_{\mathrm{V}} \in \{0, 1\}^{C_{\mathrm{V}} \times C_{\mathrm{IVT}}}$. Yellow cells (value=1) are the possible associations between the triplet and the verb. Blue cells (value=0) are the impossible associations between the triplet and the verb.
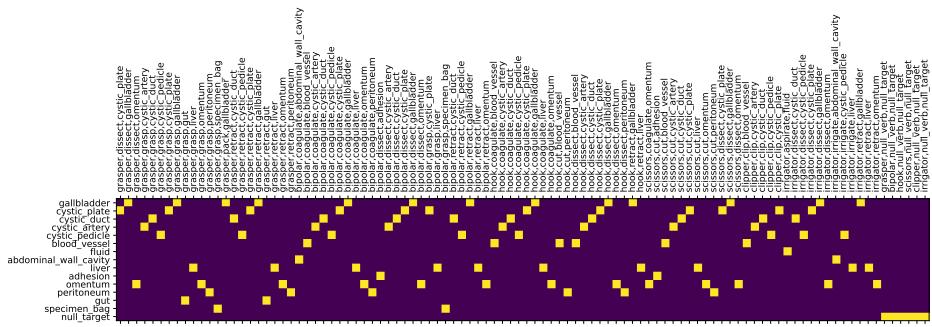
Fig. 4. Visualization of the dependency matrix $M_T \in \{0, 1\}^{C_T \times C_{IVT}}$. Yellow cells (value=1) are the possible associations between the triplet and the target. Blue cells (value=0) are the impossible associations between the triplet and the target.